ANTIOXIDANTS & REDOX SIGNALING
Volume 9, Number 8, 2007

DOI: 10.1089/ars.2007.1625

Forum Review

Measuring Oxygenation *In Vivo* with MRS/MRI—From Gas Exchange to the Cell

J.F. DUNN

ABSTRACT

Oxygen plays a major role as a substrate in metabolic processes in numerous signaling pathways, in redox metabolism, and in free radical metabolism. To study the role of oxygen in normal and pathophysiological states, methods that can be used noninvasively are required. This review examines the potential of nuclear magnetic resonance techniques to study tissue oxygenation. It is written from a systems perspective, looking at detection methods with respect to the path that oxygen takes in the mammalian system—from the lungs, through the vascular system, into the interstitial space, and finally into the cell. Methods discussed range from those that are quantifiable, such as the assessment of spin lattice relaxation time in fluorocarbon solutions, to those that are more correlative, such as assessment of lactate and high energy phosphates. Since the methods vary in their site of application, sensitivity, and specificity to the quantification of oxygen, this review provides examples of how each method has been applied. This may facilitate the reader's understanding of how to optimally apply different methods to study specific biomedical problems. *Antioxid. Redox Signal.* 9, 1157–1168.

INTRODUCTION

THE NONINVASIVE DETECTION of oxygen or "oxygenation" is of great importance for understanding both normal physiology and biochemistry of the body, as well as for understanding progression and treatment in a host of diseases. Oxygen was recognized as a key component of life since the works of Scheele, Lavoisier, and Priestley in the late 18th century. It is the fuel we burn for energy, and is also key in free radical metabolism. Historically, our capacity to measure oxygen was limited to invasive methods, such as gas chromatography or oxygen electrodes. These methods are precise, but are limited in their application to studies where some degree of tissue damage is acceptable.

The use of nuclear magnetic resonance (NMR) techniques for studying *in vivo* oxygenation has grown (119) (Table 1) in parallel with many alternate techniques. The choice of optimum methodology will be determined by a balance between available technologies and the assumptions that accompany those technologies. This review is intended as a field guide to the use of NMR to study oxygen in living systems. It will list many of the methods and attempt to provide insight as to their optimum use. As with all "anthologies," some techniques and citations may be unintentionally overlooked. The intent is that there are sufficient links to applied studies for the reader to gain access to the relevant literature.

DEFINING THE PROBLEM—THE PATH OF OXYGEN DELIVERY AND UTILIZATION

The bulk of oxygen enters the body through gas exchange at the lungs, where it is taken up into the blood and enters the circulatory system. Absorbed oxygen is transported through the vascular system to the microvasculature where it is released to cross the endothelial lining. Interstitial dissolved oxygen bathes

Department of Radiology, Physiology, and Biophysics, University of Calgary, Faculty of Medicine, Calgary, Alberta, Canada.

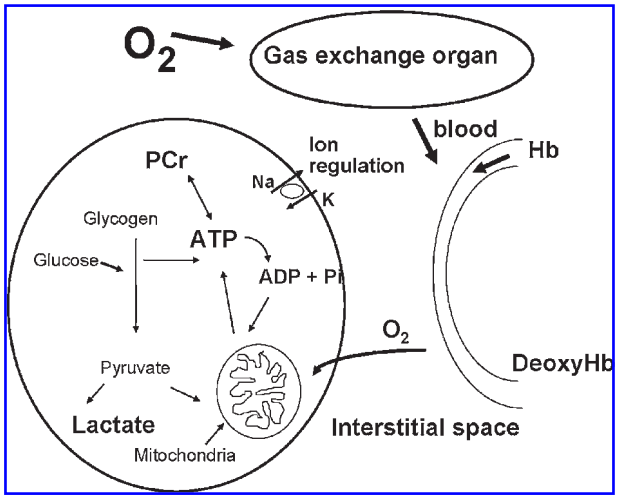

FIG. 1. The flow of oxygen from the gas exchange organ to the cell. The discussion is grouped into methods that study oxygenation in the compartments represented in this diagram. First, there is the lung, then the blood oxygen carrying pigment (hemoglobin), followed by the liquids of the plasma and the extracellular space. Methods that assess intracellular oxygenation include those which measure myoglobin, the intracellular oxygen carrying pigment, as well as those which measure metabolic factors which may correlate with oxygenation such as PCr hydrolysis, ATP, ADP, and AMP levels, lactate and proton production, ion regulation, and cell volume regulation.

the cells and follows a diffusion gradient down to the site of utilization (Fig. 1). Most of the oxygen is used in cellular metabolism. Some NMR methods assess oxygen in a fairly direct fashion by quantifying an index of concentration or partial pressure (pO_2), while most measure an index of the presence of oxygen. This gives rise to the concept of "oxygenation." This is defined as being the relative amount of "oxygen" as assessed by the impact on some specific system in the body. If the metabolite "lactate" begins to increase in the cell, it is one piece of evidence indicating the levels of oxygen have declined below those needed to maintain a more oxidative metabolic pattern. This would be evidence that tissue oxygenation has declined. If the total amount of deoxyhemoglobin decreases in an image voxel, it is also an indirect measure of oxygen, but one which again indicates that tissue oxygenation has declined. The following sections are delineated by the site of measurement along the physiological delivery pathway (Fig. 1) and by the precision by which they measure oxygen or oxygenation.

QUANTIFYING OXYGEN IN THE LUNG

Inspired O_2 can be measured with a pO_2 meter external to the subject. However, while this may be sufficient in the normal lung, there may be pathological conditions where the gas is poorly mixed in the lung, or there are residual dead spaces. In such cases, it would be useful to be able to image the pO_2 throughout the lung. Hyperpolarized ^{3}He MRI has been used for this application (24, 73). A calibration can be obtained whereby the T_1 relaxation time is proportional to the pO_2. Deninger *et al*. (24) were able to image pO_2 using this method in the human lung with an accuracy of 3%. Improvements in analysis now allow for 3D acquisition (73, 122), which should improve accuracy.

Hyperpolarized ^{3}He may be an elegant and quantifiable method, but is not readily available. An alternate method is to use perfluorocarbons to quantify pO_2. This method is more implemental in a research setting, because it is more invasive and more difficult to use in humans. The T_1 of a perfluorocarbon solution is proportional to the pO_2 of the tissue that is in contact with the solution. Perfluorocarbons have been used to obtain quantifiable pO_2 measurements. Pigs were allowed to inhale 20 ml/kg of a perfluorocarbon, and were then ventilated normally. Thus, the lung was bathed in the perfluorocarbon, but not filled with the liquid. By quantifying T_1 with a turboFLASH sequence, the authors were able to obtain regional maps of pO_2 within the liquid perfluorocarbon (51). These authors made the assumption that this represented the values in nearby tissue. Perfluorocarbons have also been infused directly into the vasculature and lung pO_2 studied (113). One of the main uncertainties here is the localization of the perfluorocarbon. The pO_2 values obtained for the lung were similar to those expected for arterial blood, indicating that the perfluorocarbon was located distal to the epithelium.

Kuethe *et al*. (65) indirectly studied oxygenation by assessing regions of variable ventilation-to-perfusion ratios within the rat lung. They imaged an inert and insoluble gas, SF6, when the rat was alternately breathing a high pO_2 or a low pO_2 mixture. They argue that when breathing the low pO_2 mixture, the distribution of the gas is uniform—providing a baseline image. When breathing a high pO_2 mixture, the distribution is sensitive to local pO_2. The ratio of images provides a regional index of the ventilation perfusion ratio.

QUANTIFYING OXYGEN IN THE BLOOD—THE OXYGEN CARRYING PIGMENT HEMOGLOBIN

Undoubtedly, one of the major advances in the study of oxygenation has been the advent of functional MRI (fMRI) (see Refs. 9, 68, 86, 93). To date, there are ~157,000 MedLine citations for fMRI. From a physiological perspective, "functional imaging" may relate to any technique that studies function *per se*. In practice, the term largely refers to studies of brain activation where changes in flow accompany changes in function. These blood flow changes result in a relative decrease in deoxyhemoglobin. Ogawa, in 1990, coined the term "blood oxygen level dependent" or BOLD imaging to define methods which are sensitive to changes in the deoxyhemoglobin content (91, 92). A major factor to consider in fMRI is that, if arterial saturation remains constant (as with almost all cognitive fMRI studies), then the venous system has a dominant influence on signal contrast (40). Thus, to localize in or near the capillary bed, one has to be careful with the choice of sequence parameters (32). There are many excellent reviews and books published on this subject and so the reader is directed to a small selection (17, 56, 60, 77, 84).

TABLE 1. EXAMPLES OF *IN VIVO* QUANTIFIED OXYGENATION MEASUREMENTS USING MRI

Region	*Oxygenation*	*Method*	*Notes*	*Citation*
Rat brain interstitial space	pO_2 = 30 mm Hg	^{19}F NMR, with T_1 quantification of perfluoro-15-crown-5-ether	PaO_2 120 mm Hg, some ventricular signal. Halothane anesthesia	31
Rat brain interstitial space	pO_2 = 15 mm Hg	^{19}F NMR, with T_1 quantification of perfluoro-15-crown-5-ether	Hypoxia, PaO_2 30–40 mm Hg, some ventricular signal. Halothane anesthesia	31
Cat cortex, mean intravascular	pO_2 = 154	^{19}F NMR, with T_1 quantification of perfluorotributylamine	Pentobarbitone anesthesia, breathing 100% oxygen	34
Intraocular region of the rabbit eye	pO_2 = 22 mm Hg	^{19}F NMR, with T_1 quantification of perfluorotributylamine	Ketamine/pancuronium anesthesia	11
Radiation induced fibrosarcoma in mice	pO_2 = 1.1–6.2 mm Hg	^{19}F NMR, with T_1 quantification of F-44E	Isoflurane anesthesia, F-44E emulsion given IV 3 days previous	50
Intraperitoneal cavity of rat	pO_2 = 7.6–33 mm Hg	^{19}F NMR, with T_1 quantification of perfluorocarbon containing alginate capsules	Chronic measurements reproduced over isoflurane anesthesia, breathing air	90
Cardiac sinus, human	Hemoglobin saturation = 41–53%	T_2 quantification of sinus blood	None, arterial assumed to be 97%	39
Cardiac, intracellular myoglobin	30% saturated	^1H of the deoxymyoglobin resonance	Isolated heart perfused with blood equilibrated to 20% oxygen	58
Skeletal muscle intracellular myoglobin	100% saturated	^1H of the deoxymyoglobin resonance	Human subjects	70, 120
Lung	pO_2 = 109 mm Hg	Hyperpolarized helium MRI	Human, initial period of breath hold	24
Cerebral spinal fluid	pO_2 = 130 mm Hg	T_1 quantification of protons	Human breathing room air, third ventricle	127

When using BOLD to study oxygenation, one needs to keep in mind that the measured value is the change in deoxyhemoglobin. Pauling (94) noted that deoxyhemoglobin is a paramagnetic substance while oxyhemoglobin was not. Thus, one can have a decrease in BOLD signal caused by an increase in deoxyhemoglobin, where that increase in deoxyhemoglobin was caused by increased cerebral blood volume (CBV) with no change in hemoglobin oxygen saturation. Since CBV increases as cerebral blood flow (CBF) increases (49), this factor may complicate the interpretation when relating BOLD data to tissue oxygenation. In the fMRI field, the use of hypercapnic breathing has become popular as a method of differentiating between changes in deoxyhemoglobin induced by changes in CBF and CBV versus those caused by changes in saturation (8, 72). One issue with respect to hypercapnia that needs to be taken into account, is that if residual hypercapnia persists, then the sensitivity to BOLD imaging will decline since CBF will already be abnormally high during the task activation (97).

With fMRI, if the increased BOLD signal that occurs with activation correlates with oxygenation, then the corresponding decrease in transverse relaxation rate (R_2*) should coincide with a decrease in deoxyhemoglobin and an increase in oxyhemoglobin. This would indicate an increase in oxygenation saturation. Many studies have shown this to be true (52, 61). Direct measurements of hemoglobin saturation within the cortical capillary bed in a rat model show increased saturation with task activation (76). When pO_2 measurements were made directly in the interstitial space with oxygen microelectrodes, increases during task activation were found (75). It is assumed that an increase in BOLD signal correlates with local activation and more oxygenated tissue. Although few studies have attempted to quantify changes in oxygenation when undertaking BOLD, work in this field has shown that oxygenation can be measured directly by quantifying R_2*. This is based on the observation that there is a predictable relationship between R_2* and deoxyhemoglobin. BOLD imaging in brain shows clear changes with increasing hypoxia caused by reducing the inspired oxygen tension (29, 91, 92). These data indicate that functional ac-

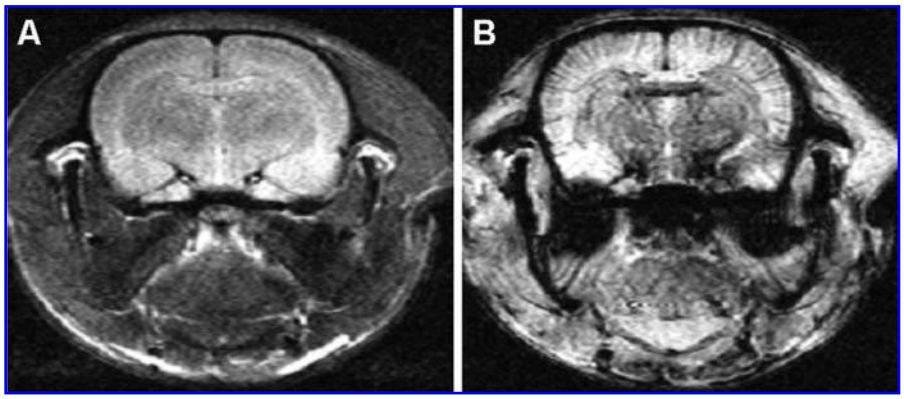

FIG. 2. The difference in sensitivity to vessel size in BOLD imaging. This MRI of a rat brain (7T) shows two images of the same slice after infusing the superparamagnetic contrast agent MION to a dose of 10 mg/kg. (**A**) Spin echo, TR/TE = 2 s/0.05 sec. (**B**) Gradient echo, TR/TE/a = 2 s/0.15 s/60°. The gradient echo sequence, which is relatively more sensitive to T_2*, shows large perforating vessels while the spin echo sequence (more sensitive to T_2) only shows constrast related to the microvasculature (unpublished data from Jeff Dunn, Marcie Roche, and Michelle Abajain).

tivation usually correlates with increased oxygenation, an increased BOLD signal, and decreased transverse relaxation rates (R_2* and R_2).

BOLD imaging has gained most of its popularity from imaging cognitive function, but it is also useful to assess oxygenation in other normal and pathological conditions. This follows since deoxyhemoglobin increases R_2 and R_2* of blood. Thulborn *et al*. (114, 115) translated the idea to that of an *in vivo* study of oxygenation, reporting the changes in blood R_2 with saturation. They also showed how kidney R_2 increased with deoxygenation. These observations supported the concept that *in vivo* studies could be undertaken that provide an index of the change in oxygenation.

One method that can be used to calibrate the change of R_2* with deoxyhemoglobin is near-infrared spectroscopy or imaging (NIR). Deoxyhemoglobin and oxyhemoglobin have characteristic absorption spectra. By quantifying the attenuation of light as it passes through the tissue, one can obtain data on the hemoglobin content and saturation using NIR (30, 83, 98).

Punwani *et al*. used NIR spectroscopy to measure changes in deoxyhemoglobin in piglet brain at 7T. The subjects were anesthetized and were exposed to a range of inspired pO_2 values to vary their arterial pO_2. The R_2* within the brain increased linearly with increased concentrations of deoxyhemoglobin (98). Jezzard *et al*. used a cranial window in a cat brain to assess hemoglobin saturation optically while simultaneously measuring changes in R_2* and also reported a good correlation (59). Both theoretical and human studies have shown that deoxyhemoglobin can be quantified if care is taken in the data collection and analysis (41, 125).

At least two studies have been undertaken where tissue pO_2 was directly measured using electron paramagnetic resonance (EPR) while R_2* was quantified. These differ from the NIR studies in that the correlation here was with interstitial oxygen levels instead of mean capillary saturation in the blood. In one study, kidney cortex and medulla pO_2 values were measured using EPR during a time-course of endotoxic shock. R_2* was quantified in parallel using a multi-echo gradient echo sequence at 7T. The changes in R_2* mirrored the direction and the time-course of the decline in pO_2 that accompanied the endotoxic shock (57). Another study examined glial tumor oxygenation in a rat model. EPR was used to measure pO_2 in parallel with MRI measurements which quantified R_2*. When rats were exposed to carbogen, a 95% O_2 and 5% CO_2 gas mixture, portions of the tumors showed an increase in oxygenation as indicated by an increased pO_2 and a decrease in R_2* (28).

An interesting observation about the BOLD signal is the impact of vessel diameter and the relationship with voxel volume and structural heterogeneity within the voxel. Mathematical modeling of the impact of changes in hemoglobin saturation show that the sensitivity of R_2 and R_2* for a given change in deoxyhemoglobin concentration varies with vessel diameter. The sensitivity of T_2 ($1/R_2$) measurements made using a spin echo sequence rises rapidly and then falls off as the vessel increases in size. The sensitivity of T_2* ($1/R_2$*) measurements made using a gradient echo sequence rises slower but remains high as vessels increase in diameter (16). A graphic example of this effect is shown in Fig. 2. The large perforating vessels are clearly seen in the gradient echo image but are not apparent in the spin echo image.

Fujita *et al*. (37) discussed some of the problems of quantifying hemoglobin with R_2 and R_2* and discussed a more accurate measure using the "reversible" R_2'. The total transverse relaxation rate in the tissue can be defined as R_2*, where $R_2^* = R_2 + R_2'$. They used a modification of the GESFIDE sequence (gradient echo sampling of FID and echo) (79) to quantify R_2' in human brain and modeled the influence of oxygenation and vessel size dependency.

The fact that both T_2 and T_2* change with hemoglobin saturation leads to many useful applications. In cardiac imaging, one may want to know the saturation in large vessels or even in the ventricles. It is difficult to measure T_2* due to the motion and large liquid tissue interfaces. In this case, T_2 quantification has been used to measure saturation in the coronary sinus (39). Early cardiac BOLD work showed that one could obtain a good estimate of tissue saturation in the septum of an arrested heart with T_2 measurements (7).

If one is interested in studying angiogenesis, and wants to limit the detection sensitivity to the microvasculature, T_2 quantification is also the method of choice over that of T_2*. Angio-

genesis has been measured in normal brain where a hypoxia stimulus was used to stimulate the growth of the microvasculature (26). Further, by taking advantage of the relative differences in sensitivity of T_2 and T_2* imaging to vessel size, both parameters can be measured to generate a vessel size dependency image (25). These methods all arise from applying BOLD imaging in novel ways.

There is extensive literature on the use of BOLD imaging to study tumor oxygenation (3, 5, 28, 44, 45, 54, 102). There is significant interest in developing techniques to grade a tumor with respect to its oxygenation because very hypoxic tumors are insensitive to radiation treatment. Furthermore, it would be helpful to use BOLD to determine if a tumor reoxygenation occurred in response to therapy. One example of this application showed a 40% increase in the gradient echo image intensity when carbogen was inhaled (102). In another study, BOLD imaging showed improved tumor oxygenation when the oxyhemoglobin dissociation curve was shifted (53). BOLD imaging has also been applied to study tumor oxygenation in human studies. Griffiths *et al.* (48) used MRI to study head and neck tumors in patients before and after carbogen breathing. They identified a tumor in the neck of a patient that was missed by conventional MRI. Other methods have been used and the reader is directed to the review by (126).

An important point is that heterogeneity within the voxel of signal from vessels and non-vessels can give rise to a frequency shift as well as a change in relaxation rate. Karczmar's group took advantage of this phenomenon to study the heterogeneity of tumor response to changes in inspired oxygen. They developed a spectral-spatial method where they simultaneously quantified the frequency shift and relaxation rate. This study clearly shows that there was intravoxel heterogeneity in the BOLD response in tumors (3). They also undertook a quantification study where they correlated pO_2 measured with microelectrodes in the tumor to the changes in relaxation rate (4). In another study, they measured perfluorocarbon-based measurements of pO_2 and confirmed that the changes in tissue pO_2 correlated with R_2* measurements (38). The spectral-spatial method correlates with changes in the hypoxic fraction, a radiation therapy based assessment of oxygenation (5).

These data using spectral-spatial imaging help explain the observation that the decline in signal intensity with echo time in a gradient echo study may not follow a simple exponential function. This decay curve is used to calculate the R_2*. In a study of normal brain, the relaxation rate appears to follow an exponential function in most voxels. However, in pathological states such as tumors, this relationship can become very complex—making it more difficult to quantify deoxyhemoglobin using R_2* methods (28). One can hypothesize that the larger, more tortuous vessels observed in the rat 9L glioma model influence the heterogeneity of relaxation rates within a voxel and contribute to the nonexponential signal decay patterns observed in the tumors (28).

Skeletal muscle physiologists have also used BOLD to study oxygenation (69, 71, 87, 89). BOLD is particularly suited to the study of peripheral vascular disease. There were significant differences in R_2* changes in response to a reversible occlusion in a patient group, as compared with controls (71). A study of rat kidney during endotoxic shock used BOLD MRI to measure relative changes in oxygenation in the cortex and medulla over time (57). Since the kidney is almost 15% blood by volume, BOLD imaging could have a major impact on the physiological assessment of this organ (81). The BOLD literature is extensive enough that it is possible to find examples of its application in almost all organ systems of the body. Clearly, this method of assessing oxygenation is still growing in its relative importance.

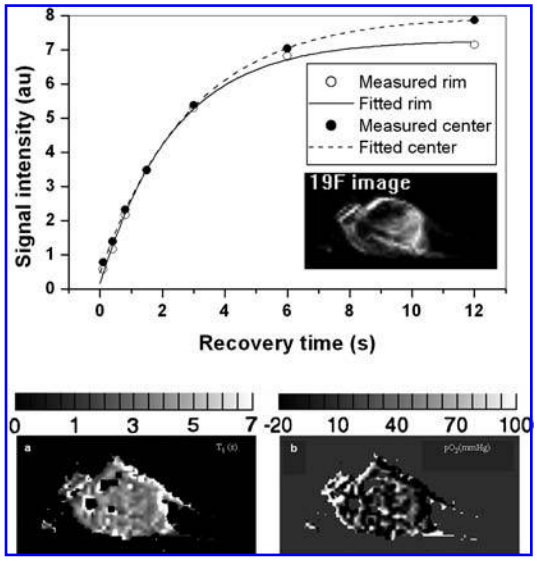

FIG. 3. ^{19}F-based pO_2 map in a tumor. *Top*: A plot of signal intensity vs. recovery time in the inversion recovery sequence used to measure T_1. The curves were obtained for small ROIs at the tumor rim and tumor center. The *insert* shows the gradient echo. ^{19}F image of the subcutaneous tumor, which shows where there are pixels which contain ^{19}F. Only these pixels will provide data for the pO_2 map. *Bottom*: T_1 map and pO_2 map derived for those pixels where goodness-of-fit was better than 0.95. The scale bar is given above the corresponding image. The displayed FOV is 40 mm x 20 mm. Reproduced with permission from Ref. 37.

FROM THE BLOOD TO THE CELL—ASSESSING OXYGEN IN LIQUIDS

After oxygen arrives in the capillary bed, it crosses the endothelial cell lining by diffusion down concentration gradients to the site of utilization—which is predominantly in the mitochondria. Methods that quantify oxygen in solution can be used to assess oxygenation along this path of diffusion.

Perfluorocarbons, discussed above for use in the lung, have a T_1 that is oxygen sensitive and can be safely infused to fairly high concentrations. Their final site of distribution determines the location of the measured pO_2 (Fig. 3). If the infusion is done hours to days before the imaging, then the agent will be sequestered into the tissue (23, 37). If the study is done soon after injection, then most of the perfluorocarbon will be in the plasma and the value returned will be an average of the pO_2 within the vessels in the voxel. That value will be weighted by the relative distribution of veins, arteries, and capillaries. At

later time points after injection, perfluorocarbons may be transported to an extravascular site that probably varies with tissue and pathological state (37). One of the earlier uses of this method was in 1988 where perfluorocarbon (perfluortributylamine) infusion was used to study pO_2 in brain (34). Cats were anesthetized with pentabarbitone and allowed to breathe 100% oxygen. The pO_2 measured by this method was 186 mm Hg in the carotid artery and pO_2 distribution histogram was presented. Improvements in the method resulted in better cross-sectional maps of rat brain pO_2 (10).

Oxygenation in animal models of cancer have been studied at least since 1993 using perfluorcarbons, when it was shown that nicotinamide can increase animal tumor pO_2 by a mean value of 4.5 mm Hg (50). Hexafluorobenzene has been proposed as a good perfluorocarbon to use since it is readily available and can be used to assess heterogeneity of pO_2 in animal tumor models (55, 82). Complex perfluorocarbons often have multiple fluorine resonances which can make it more difficult to image. Ideally, the multiple fluorines will have similar local environments, resulting in the compound having fewer resonances but more amplitude per resonance, thus increasing sensitivity. The compound PTBD (perfluoro-2,2,2′,2′-tetramethyl-4,4′-bis(1,3-dioxolane)) was studied and demonstrated an increase in sensitivity (108).

Oxygenation in regions of the body where there are pools of liquid can also be studied with perfluorocarbons. The vitreous space in the eye is an excellent example. The compounds can be injected directly to the site of interest. In1991, Berkowitz injected perfluorotributylamine into the vitreous and measured a value of 22 ± 4.7 mm Hg (mean $\pm$ SD) in the eye (11). To measure pO_2 in brain, perfluorocarbon can be directly infused into the ventricles and will diffuse into the interstitial space. Duong *et al*. used this method to correlate changes in CBF measured with MRI to the changes in local tissue pO_2 during acute hypoxia, hyperoxia, and hypercapnia (31).

An extension of the application to study pO_2 in areas of liquid pools is one where perfluorocarbons have been incorporated into implantable materials. In one instance, alginate capsules were implanted in rat kidney, skeletal muscle and the peritoneal cavity. Chronic measurements of pO_2 were made within the capsules over months (90).

In a novel application of perfluorocarbons, the vascular volume fraction was calculated from measuring the respective components of the T1 decay. The authors argued that if the volume measured by a given T1 fraction was relatively hypoxic, then that volume corresponded to the venous blood, while the more oxic volume related to arterial blood. Using this method, they reported an arterial volume fraction of ~30% (33).

In theory, the perfluorocarbon measurement of intravascular pO_2 can be used to estimate the total oxygen in the blood. One would use knowledge of the oxyhemoglobin dissociation curve and the pH. It should be noted that this curve is not the same for humans and rodents. Blood gas analyzers which calculate hemoglobin saturation based on pH and pO_2 use a human form of the oxyhemoglobin dissociation curve. One can use published data for rodent blood if a conversion is required (18).

Contrast agents have been proposed for measuring oxygen in solution. Selected spin-trapping agents, developed for EPR, have been used in combination with NMR. For an excellent review on the subject see Ref. 12. For instance, the dithiocarbamate "Fe(II)-NO" complex results from the trapping of nitric oxide (12). The T_1 and T_2 values of protons in MRI around the complex decrease with binding. As a result, binding causes signal enhancement on a T1-weighted MRI. MR spectroscopy can be used to detect resonances that appear with radical spin adduct degradation and reduction (12). Although this is not a direct measure of oxygen, the reaction and the physiology associated with NO production are both influenced by oxygenation.

If EPR and NMR can be used in parallel, then oxygen-sensitive nitroxides make a very interesting contrast agent. When being measured with EPR, they can report local pO_2. Then, the subject can be moved to the MRI and both the location and the relative perfusion in that area can be assessed by T1w MRI as the nitroxide will shorten the T_1 of the surrounding protons (42).

The use of nitroxides for a more direct measurement of pO_2 using MRI was proposed in 1985 (110). Here the concept was that changes in oxygenation and redox metabolism in the local environment would change the reduction rate for nitroxides. The nitroxide is relatively stable under oxidative conditions. When oxygen levels fall, it is reversibly converted into a nonparamagnetic product (111). Thus, the nitroxide has the potential for being an oxygenation sensitive contrast agent.

Spectroscopy can also be used to monitor nitroxide products. An example of this is the study using 5-diisopropoxy-phosphoryl-5-methyl-1-pyrroline-N-oxide (DIPPMPO). Stable ^{31}P-NMR visible radical adducts are formed when DIPPMPO reacts with free radicals (6). NMR spectroscopy can be used to quantify the time-course of the appearance of new resonances, which correspond to the time-course of production and reaction of the free radicals.

A very remarkable contrast-related method that also involves cross-over between EPR and NMR is termed Overhauser-enhanced MRI (OMRI) (64) or proton electron double resonance imaging (PEDRI) (78). With OMRI, EPR excitation of an infused EPR-sensitive contrast agent precedes the MRI acquisition. Proton enhancement in the MRI occurs through the nuclear Overhauser effect. Low field strengths are used due to the high frequencies of EPR irradiation. These field strengths (*e.g.*, 0.02T) typically result in very poor quality MR images. However, using OMRI enhancement was provided by EPR irradiation of a trityl paramagnetic contrast agent (1 mm/kg dose) and a rat vascular image was made with better quality than that obtained on many 1.5T MRI systems (46). Enhancement has been reported of ~60 times in the signal to noise over that of the nonirradiated MR image (47). Since the line width of such contrast agents is proportional to pO_2, appropriate calibrations can be made to generate pO_2 sensitive images in MRI (47, 64). In PEDRI, the MRI field strength is cycled down to an appropriate field for EPR irradiation, and then ramped up again for MRI detection. The advantages of these techniques are the very low magnetic fields used and the remarkable capability to generate MR images that have oxygen sensitive contrast.

One of the earliest methods for detecting changes in oxygenation of a fluid using NMR involved the simple quantification of T_1. The T_1 of blood will change in proportion to both hematocrit and oxygen saturation (107). All else being equal, the T_1 of tissues relates to the oxygen levels in the animal (112). This study showed that T_1 values were reduced in some organ systems when the animal breathed 100% oxygen. The lack of a universal decline in T1 indicates that either all organ systems

do not have an increase in oxygenation when breathing 100% oxygen, or the method is not very specific. It may be that when targeting a more limited problem, this method may be more robust. For instance, changes in proton T_1 have been used to monitor oxygenation in the cerebrospinal fluid in the brain of human subjects who were breathing room air or 100% O_2. The brain's ventricular pO_2 was quantified and shown to be both variable throughout the brain as well as sensitive to changes in inspired O_2 (127).

Direct measurement of T_1 can also be used to measure blood oxygenation. The R_1 ($1/T_1$) of left-cardioventricular blood increased by 12% as inspired oxygen was changed from 21% to 100% (117). Hyperpolarized Xe is being increasingly used in MRI. The T_1 of Xe in blood is nonlinearly proportional to local oxygenation. The changes in relaxation rate appear to be influenced by conformational changes in hemoglobin and so may provide an index of blood saturation (124).

A method for studying oxygenation using intermolecular zero-quantum coherences was proposed in 1998. Here, contrast is related to long-range dipolar couplings and is based on magnetic susceptibility. This method has promise for assessing oxygen concentrations, perhaps even directly in solution (121). Intramolecular double quantum coherences have also been studied as a measure of task activation in brain. In such activation studies, the contrast appears sensitive to susceptibility changes, indicating that the method may relate to deoxyhemoglobin (128, 129) although this remains speculative (104).

QUANTIFYING OXYGEN IN THE CELL—MYOGLOBIN

There is a very high concentration of myoglobin in heart and skeletal muscle—making it possible to use MR spectroscopy for detection. Proton spectra of myoglobin show a characteristic resonance of the N-delta proton of the F8 proximal histidine (120). Thus, ^1H spectroscopy can be used to monitor intracellular pO_2 through inference of the oxygen binding curve of myoglobin. In human muscle, intracellular pO_2 at rest was 34 mm Hg and declined to 23 mm Hg with reduction in inspired O_2 (101). In isolated perfused rat hearts, this method showed that intracellular pO_2 can be maintained at a relatively constant value as work loads in the heart are changed over an eightfold range (58). NIR studies done simultaneously with ^1H MRS in human skeletal muscle have been used to validate this method. Ischemia in human gastrocnemeus muscle was induced with a cuff. The desaturation observed with NIR was coincident with an increase in the proximal histidyl deoxyHb resonance (116).

Proton spectroscopy can also be used to detect changes in oxymyoglobin. The methyl group of VAL-E11 has a chemical shift that is saturation dependent and ranges from -2.76 to -2.40 ppm (63). A recent study examined the role of facilitated diffusion. Oxygen can diffuse directly through the fluid in the cell at a certain diffusion rate. In theory, since diffusion of myoglobin may occur independently of that of dissolved oxygen, the maximum diffusion rate of oxygen will be the sum of the two processes. This role of myoglobin to enhance the diffusion rate is termed "facilitated diffusion." This study inhibited facilitated diffusion by using carbon monoxide to inhibit the oxygen carrying capacity of myoglobin and compared the oxygen uptake in a working heart to that measured during acute hypoxia alone. They found no evidence that inhibition of facilitated diffusion resulted in impaired oxygen utilization(20).

Although the BOLD effect was described with respect to blood and hemoglobin, it also applies to muscle and myoglobin. In both skeletal and cardiac muscle, the interpretation is made more complex by the presence of both hemoglobin in blood and myoglobin in myocytes within a given voxel. Since the p50 of myoglobin is much less than that of hemoglobin, it has been suggested that hemoglobin saturation would decline, and deoxyhemoglobin content would increase before there were any changes in myoglobin saturation. A study measuring R_2* while obtaining ^1H spectra indeed showed that there were measurable increases in R_2* with exercise before there were observed increases in deoxymyoglobin (69).

QUANTIFYING OXYGEN IN THE CELL—CORRELATES OF OXYGENATION

It is theoretically possible to monitor intracellular processes which, in themselves, have an oxygen sensitivity and thereby gain some insight into cellular oxygenation. Inhibition of these processes can often be correlated with a reduction in cellular oxygenation.

Energy production in most cells is linked to the availability of oxygen. One of the first and most widely used NMR methods for studying cellular energy status was ^{31}P-NMR spectroscopy (1, 99). Arguments based on modeling oxidative pathways as well as on empirical measurements led to the suggestion that inorganic Pi concentration relates to mitochondrial redox state (85), and to the balance between energy utilization and oxygen delivery. It follows that Pi or the ratio of Pi to total phosphate has often been used as an indirect indicator of oxygenation.

In some conditions, this assumption has merit. Tumor metabolism has often been studied with ^{31}P-NMR. In one example, a potential inducer of hypoxia, hydralazine, was given to mice with subcutaneous tumors while ^{31}P-NMR was used to monitor the time-course of changes in high energy phosphates and Pi. At discrete time-points, the hypoxic fraction of the tumors was measured as an index of tissue oxygen. The increase in Pi correlated well with the increase in hypoxic fraction (27). When localized ^{31}P spectroscopy was used, it was noted that there was regional heterogeneity in the response (13).

Using an animal model of a mammary carcinoma, ^{31}P-NMR was undertaken along with pO_2 measurements made using an oxygen electrode, before and after radiation therapy. The study investigated the postradiation reoxygenation phenomenon and showed that an increase in high energy phosphates (NTP) coincided with increased pO_2 (62).

A high degree of variability in measurements of pO_2 in tumors often results, regardless of the method used. Since the radiation sensitivity declines with hypoxia and occurs predominantly with pO_2 values <10 mm Hg, correlation of the tumor response to hypoxia usually needs only to identify regions which are hypoxic <10 mm Hg. As a result, many studies group the pO_2 values into bins, providing a better correlation but less precision as to the actual pO_2 value. In such a study tumors showed increased numbers of low pO_2 readings after irradia-

tion as well as significantly lower values for PCr/Pi and NTP/PI (118).

The intracellular pH can also be measured with ^{31}P-NMR and, since anaerobic lactate production often coincides with acidification, may provide an index of hypoxia. In a study of solid tumors, adenylate concentrations remained relatively constant until very low pO_2 values, ~100 mm Hg. At this point, the cells also began to acidify (107).

These types of studies have been very important in determining the pathophysiology of specific tumor types and for making the argument that tumor hypoxia is coincident with radiation insensitivity.

There was widespread interest in using ^{31}P spectroscopy to study tumor oxygenation to provide an index of radiation sensitivity. One key study used an *in vivo* tumor model where the inflow and out flow vessels were cannulated to allow for control of flow and delivery of both oxygen and glucose. They reported little or no change in the ^{31}P spectra when oxygen delivery was reduced. They did observe major reductions in energy metabolism when flow was reduced (35).

Vaupel *et al*. also found that tumor high energy phosphates were constant over a wide range of pO_2 values, but did decline at very low values of oxygenation in solid tumor models. This indicates that ^{31}P-NMR may provide a correlative index as to whether tumors have declined below a critical oxygen tension for support of energy metabolism (117, 118). Although this conflicts with the lack of oxygen sensitivity in the mammary tumor model of Eskey (35), it is consistent with the presence of a similarly observed critical oxygen tension in mammalian brain (103). NIR studies of hemoglobin saturation in brain also show significant decline in oxygen levels before there is an impact on energy metabolism (109).

When rats were exposed to graded hypoxia, the pO_2 in brain showed a proportionate decline in pO_2 as measured by EPR oximetry. The high energy phosphates were stable until a critical point indicating that, not surprisingly, there is a nonlinear relationship between tissue oxygenation and high energy phosphate content (103). In ischemia, high energy phosphates are a sensitive measure of metabolic decline (85).

Although in earlier studies it was shown that tumor ischemia related to energetics (36), using cell lines with differing hypoxic fractions, it was shown that the response of energy metabolism to hypoxia was not predictable (43). These and other studies led to significant discussions on the subject. The conclusion in tumor studies is that only under specific conditions can ^{31}P data be used to indicate hypoxia. These would be where independent validation has been made, or where knowledge of the physiology and biochemistry of the system can be applied. Measurement of tumor oxygenation as an index of treatment response is a growing field in which noninvasive methods such as NMR will play an important role.

Phosphorus NMR spectroscopy has found many applications for assessing metabolism and oxygenation. This includes monitoring skin of people with diabetes where it was shown that ingestion of nicotine reduced the PCr/Pi ratio in skin, ostensibly due to vasoconstriction and ischemia (107).

However, ^{31}P spectroscopy does not always correlate well with oxygenation. Various groups of human muscle groups were studied during and after 5 min of ischemia–reperfusion. Oxygenation was measured with NIR, Na-NMR was used to study shifts in ion concentrations, and ^{31}P-NMR spectroscopy was performed. There were no measurable changes in the high energy phosphates under conditions where energy metabolism increased enough to cause significant reductions in oxygenation (14).

Lactate is a metabolite linked to anaerobic glycolysis, and so may change in concentration with tissue oxygenation—or with changes in the balance of oxidative versus nonoxidative energy production. Since lactate dehydrogenase is an equilibrium enzyme, the cellular concentration of lactate also depends on local pH and redox potential. Proton spectra have shown that lactate increases in the rat brain during acute hypoxia where the PaO_2 was $<$54 mm Hg. However, the lactate resonance did not return to baseline upon reoxygenation (95), indicating that the existence of lactate is not always concurrent with hypoxia. There are some notable exceptions where lactate will occur during "normoxia" such as with a toxoplasmosis infection (19). When comparing the ^{1}H spectra of brains from different strains of mice, relative increases in lactate did not correlate with hypoxia (105).

In stroke/ischemia studies where lactate has been measured, it always shows an increase. There is extensive literature on this subject (80). The presence of lactate in pediatric disorders reflects poor outcome (106), but again it is not clear to what level there is concurrent hypoxia.

Carbon-13 NMR has been used extensively to study cellular metabolism and carbon flux. As with ^{1}H- and ^{31}P-NMR spectroscopy, the correlation with hypoxia will depend significantly on the metabolic status. One can fall back on decades of research into the regulation of oxidative versus glycolytic carbon flux with respect to interpreting the ^{13}C flux data. As expected, glycolytic flux does increase with progressive hypoxia as shown in a neuronal cell culture study (88).

As energy stores decline in a cell, so does the capacity to maintain ionic electrochemical concentration gradients and to regulate water balance. As a result, cells often swell in the presence of acute hypoxia or the combination of hypoxia and ischemia. There are a range of NMR based methods to study these parameters. Ion contents and fluxes can be assessed directly with ^{23}Na or ^{39}K NMR (2, 21, 100). Potassium content increased with ischemia in the heart and then returned to baseline during reperfusion (100). It has already been noted that energy status of the cell relates to oxygenation in a complex fashion. Since ionic regulation would not be impaired until energy production was inhibited, the changes observed in ^{23}Na do not occur immediately upon the onset of hypoxia or ischemia (15, 21) but abnormal regulation is consistent with a cell under stress.

Studies using ^{87}Rb are useful as the ion is an NMR sensitive cogenor for potassium and can be used to study potassium flux through Na,K-ATPase. Cardiac studies have shown that Rb flux declines with ischemia and correlates with a fall in ATP (21, 66). In a similar type of study, ^{7}Li was used as a cogener for Na transport in isolated hearts. Hearts were pre-loaded with ^{7}Li and the washout of the Li monitored (67)

CORRELATING OXYGENATION WITH FLOW

In vertebrate systems, most of the oxygen is delivered to the tissues via the blood. It is not surprising that flow itself, the

process of oxygen delivery, correlates in many cases to tissue oxygenation. The oxygen levels in the tissue are a balance between flow (or delivery) and utilization. If the two were perfectly matched, one might imagine that tissue oxygenation could be independent of flow. However, it has already been noted that when flow increases during functional brain activation, the brain interstitial pO_2 increases as does the blood oxygenation (61, 75). Under anesthesia, the pO_2 in the brain correlates with CBF once pO_2 has declined to a threshold (31, 74). In the ischemic brain the reduction in flow correlates with a reduction in tissue pO_2. This is caused by the fact that, in the first case, the tissue is functioning normally and physiological mechanisms are available to ensure that substrates are delivered when required. In the latter case, the ischemic event results in a limitation of substrate delivery and the tissue oxygen is used to the maximum amount possible based on the kinetics of the enzymes for oxidative metabolism.

The relationship between flow and oxygenation is tissue specific and will vary with pathological condition. A review of flow MRI is beyond the scope of this article but suffice it to say that in a given organ system, there is likely to be a relationship between flow and oxygenation that can be capitalized upon to gain an index of oxygenation. The reader is directed to texts or to a selection of review articles (22, 96, 123).

CONCLUSIONS

With the growing availability of NMR techniques that can be applied to the study of oxygen-related mechanisms and disease processes, comes a growing pantheon of methods that can be applied to a particular study. The methods range in their site of application and their relative capacity to quantify the results. They include imaging and spectroscopic methods and a range of NMR visible nuclei.

ACKNOWLEDGMENTS

This work was partially supported by a National Institutes of Health RO1 EB002085, by the Canadian Institutes of Health Research FIN 79260, and by the Alberta Heritage Foundation.

ABBREVIATIONS

BOLD, Blood Oxygen Level Dependent. This refers to the MRI methods that are sensitive to deoxyhemoglobin; CBV, cerebral blood volume; deoxyHb, deoxyhemoglobin; EPR, electron paramagnetic resonance; fMRI, functional MRI; Hb, hemoglobin; MR, magnetic resonance; MRI, magnetic resonance imaging; NIR, near-infrared; NMR, nuclear magnetic resonance; NTP, nucleoside triphosphates; PCr, phosphocreatine; p50, partial pressure of oxygen at which one achieves $^1/_2$ saturation of hemoglobin or myoglobin; Pa O_2, arterial partial pressure of oxygen; Pi, inorganic phosphate; pO_2, partial pressure of oxygen; R_1, longitudinal or spin-lattice relaxation rate; R_2, transverse or spin-spin relaxation rate; R_2*, total transverse rate; T_1, longitudinal or spin-lattice relaxation time; T_2, transverse or spin-spin relaxation time constant; T_2*, total transverse time constant; T_2', reversible transverse time constant; TE, echo time; TR, repetition time.

REFERENCES

1. Ackerman JJ, Grove TH, Wong GG, Gadian DG, and Radda GK. Mapping of metabolites in whole animals by 31P NMR using surface coils. *Nature* 283: 167–70, 1980.
2. Adam WR, Koretsky AP, and Weiner MW. Measurement of tissue potassium *in vivo* using 39K nuclear magnetic resonance. *Biophys J* 51: 265–71, 1987.
3. Al–Hallaq HA, Fan X, Zamora M, River JN, Moulder JE, and Karczmar GS. Spectrally inhomogeneous BOLD contrast changes detected in rodent tumors with high spectral and spatial resolution MRI. *NMR Biomed* 15: 28–36, 2002.
4. Al–Hallaq HA, River JN, Zamora M, Oikawa H, and Karczmar GS. Correlation of magnetic resonance and oxygen microelectrode measurements of carbogen-induced changes in tumor oxygenation. *Int J Radiat Oncol Biol Phys* 41: 151–159, 1998.
5. Al–Hallaq HA, Zamora M, Fish BL, Farrell A, Moulder JE, and Karczmar GS. MRI measurements correctly predict the relative effects of tumor oxygenating agents on hypoxic fraction in rodent BA1112 tumors. *Int J Radiat Oncol Biol Phys* 47: 481–488, 2000.
6. Argyropoulos DS, Li H, Gaspar AR, Smith K, Lucia LA, and Rojas OJ. Quantitative ^{31}P NMR detection of oxygen-centered and carbon-centered radical species. *Bioorg Med Chem* 14: 4017–4028, 2006.
7. Atalay MK, Reeder SB, Zerhouni EA, and Forder JR. Blood oxygenation dependence of T1 and T2 in the isolated, perfused rabbit heart at 4.7T. *Magn Reson Med* 34: 623–627, 1995.
8. Bandettini PA and Wong EC. A hypercapnia-based normalization method for improved spatial localization of human brain activation with fMRI. *NMR Biomed* 10: 197–203, 1997.
9. Bandettini PA, Wong EC, Hinks RS, Tikofsky RS, and Hyde JS. Time course EPI of human brain function during task activation. *Magn Reson Med* 25: 390–397, 1992.
10. Bellemann ME, Bruckner J, Peschke P, Brix G, and Mason RP. [Quantification and visualization of oxygen partial pressure *in vivo* by 19F NMR imaging of perfluorocarbons]. *Biomed Tech (Berl)* 47 Suppl 1 Pt 1: 451–454, 2002.
11. Berkowitz BA, Wilson CA, Hatchell DL, and London RE. Quantitative determination of the partial oxygen pressure in the vitrectomized rabbit eye *in vivo* using 19F NMR. *Magn Reson Med* 21: 233–241, 1991.
12. Berliner LJ, Khramtsov V, Fujii H, and Clanton TL. Unique *in vivo* applications of spin traps. *Free Rad Biol Med* 30: 489–499, 2001.
13. Bhujwalla ZM, Blackband SJ, Wehrle JP, and Glickson JD. Spatial heterogeneity of the metabolic response of RIF-1 tumors to a vasoactive agent evaluated *in vivo* by one-dimensional 31P chemical-shift imaging. *Magn Reson Med* 26: 308–312, 1992.
14. Binzoni T, Quaresima V, Barattelli G, Hiltbrand E, Gurke L, Terrier F, Cerretelli P, and Ferrari M. Energy metabolism and interstitial fluid displacement in human gastrocnemius during short ischemic cycles. *J Appl Physiol* 85: 1244–1251, 1998.
15. Bowers JL, Lanir A, Metz KR, Kruskal JB, Lee RG, Balschi J, Federman M, Khettry U, and Clouse ME. 23Na- and 31P-NMR studies of perfused mouse liver during nitrogen hypoxia. *Am J Physiol* 262: G636–44, 1992.
16. Boxerman JL, Hamberg LM, Rosen BR, and Weisskoff RM. MR contrast due to intravascular magnetic susceptibility perturbations. *Magn Reson Med* 34: 555–566, 1995.
17. Buxton RB, Uludag K, Dubowitz DJ, and Liu TT. Modeling the hemodynamic response to brain activation. *Neuroimage* 23 Suppl 1: S220–233, 2004.
18. Cartheuser CF. Standard and pH-affected hemoglobin-O_2 binding curves of Sprague-Dawley rats under normal and shifted P50 conditions. *Comp Biochem Physiol Comp Physiol* 106: 775–782, 1993.

19. Chang L, Miller BL, McBride D, Cornford M, Oropilla G, Buchthal S, Chiang F, Aronow H, and Ernst T. Brain lesions in patients with AIDS: H-1 MR spectroscopy. *Radiology* 197: 525–531, 1995.
20. Chung Y, Huang SJ, Glabe A, and Jue T. Implication of CO inactivation on myoglobin function. *Am J Physiol Cell Physiol* 290: C1616–1624, 2006.
21. Cross HR, Radda GK, and Clarke K. The role of Na+/K+ ATPase activity during low flow ischemia in preventing myocardial injury: a 31P, 23Na and 87Rb NMR spectroscopic study. *Magn Reson Med* 34: 673–685, 1995.
22. Cuocolo A, Acampa W, Imbriaco M, De Luca N, Iovino GL, and Salvatore M. The many ways to myocardial perfusion imaging. *Quart J Nuc Med* 49: 4–18, 2005.
23. Dardzinski BJ and Sotak CH. Rapid tissue oxygen tension mapping using ^{19}F inversion-recovery echo-planar imaging of perfluoro-15-crown-5-ether. *Magn Reson Med* 32: 88–97, 1994.
24. Deninger AJ, Eberle B, Ebert M, Grossmann T, Heil W, Kauczor H, Lauer L, Markstaller K, Otten E, Schmiedeskamp J, Schreiber W, Surkau R, Thelen M, and Weiler N. Quantification of regional intrapulmonary oxygen partial pressure evolution during apnea by ^{3}He MRI. *J Magn Reson* 141: 207–216, 1999.
25. Dennie J, Mandeville JB, Boxerman JL, Packard SD, Rosen BR, and Weisskoff RM. NMR imaging of changes in vascular morphology due to tumor angiogenesis. *Magn Reson Med* 40: 793–799, 1998.
26. Dunn J, Roche M, Springett R, Abajian M, Merlis J, Daghlian C, Lu S, and Makki M. Monitoring angiogenesis in brain using steady-state quantification of DeltaR2 with MION infusion. *Magn Reson Med* 51: 55–61, 2004.
27. Dunn JF, Frostick S, Adams GE, Stratford IJ, Howells N, Hogan G, and Radda GK. Induction of tumour hypoxia by a vasoactive agent. A combined NMR and radiobiological study. *FEBS Lett* 249: 343–347, 1989.
28. Dunn JF, O'Hara JA, Zaim–Wadghiri Y, Lei H, Meyerand ME, Grinberg OY, Hou H, Hoopes PJ, Demidenko E, and Swartz HM. Changes in oxygenation of intracranial tumors with carbogen: A BOLD MRI and EPR oximetry study. *J Magn Reson* 16: 511–521, 2002.
29. Dunn JF, Wadghiri YZ, and Meyerand ME. Regional heterogeneity in the brain's response to hypoxia measured using BOLD MR imaging. *Magn Reson Med* 41: 850–854, 1999.
30. Dunn JF, Zaim Wadghiri Y, and Kida I. BOLD MRI vs. NIR spectroscopy: will the best technique come forward? *Adv Exp Med Biol* 454: 103–113, 1998.
31. Duong TQ, Iadecola C, and Kim SG. Effect of hyperoxia, hypercapnia, and hypoxia on cerebral interstitial oxygen tension and cerebral blood flow. *Magn Reson Med* 45: 61–70, 2001.
32. Duong TQ, Kim DS, Ugurbil K, and Kim SG. Localized cerebral blood flow response at submillimeter columnar resolution. *Proc Natl Acad Sci USA* 98: 10904–10909, 2001.
33. Duong TQ and Kim SG. *In vivo* MR measurements of regional arterial and venous blood volume fractions in intact rat brain. *Magn Reson Med* 43: 393-402, 2000.
34. Eidelberg D, Johnson G, Barnes D, Tofts PS, Delpy D, Plummer D, and McDonald WI. 19F NMR imaging of blood oxygenation in the brain. *Magn Reson Med* 6: 344–352, 1988.
35. Eskey CJ. Role of oxygen vs. glucose in energy metabolism in a mammary carcinoma perfused *ex vivo*: direct measurment by 31P NMR. *Proc Natl Acad Sci USA* 90: 2646–2650, 1993.
36. Evelhoch JL, Sapareto SA, Nussbaum GH, and Ackerman JJ. Correlations between ^{31}P NMR spectroscopy and ^{15}O perfusion measurements in the RIF-1 murine tumor *in vivo*. *Rad Res* 106: 122-131, 1986.
37. Fan X, River JN, Muresan AS, Popescu C, Zamora M, Culp RM, and Karczmar GS. MRI of perfluorocarbon emulsion kinetics in rodent mammary tumours. *Phys Med Biol* 51: 211–220, 2006.
38. Fan X, River JN, Zamora M, Al–Hallaq HA, and Karczmar GS. Effect of carbogen on tumor oxygenation: combined fluorine-19 and proton MRI measurements. *Int J Radiat Oncol Biol Phys* 54: 1202–1209, 2002.
39. Foltz WD, Merchant N, Downar E, Stainsby JA, and Wright GA. Coronary venous oximetry using MRI. *Magn Reson Med* 42: 837–848, 1999.
40. Frahm J, Klaus-Dietmar M, Hanicke W, Kleinschmidt A, and Boecker H. Brain or vein-oxygenation or flow? On signal physiology in functional MRI of human brain activation. *NMR Biomed* 7: 45–53, 1994.
41. Fujita N, Shinohara M, Tanaka H, Yutani K, Nakamura H, and Murase K. Quantitative mapping of cerebral deoxyhemoglobin content using MR imaging. *Neuroimage* 20: 2071–2083, 2003.
42. Gallez B, Bacic G, Dunn JF, Goda F, Jiang J, O'Hara JA, and Swartz HM. Use of nitroxides for assessing perfusion, oxygenation, and viability of tissues: *in vivo* EPR and MRI studies. *Magn Reson Med* 35: 97–106, 1996.
43. Gerweck LE, Koutcher JA, Zaidi ST, and Seneviratne T. Energy status in the murine FSaII and MCaIV tumors under aerobic and hypoxic conditions: an *in vivo* and *in vitro* analysis. *Int J Radiat Oncol Biol Phys* 23: 557–561, 1992.
44. Gilad AA, Israely T, Dafni H, Meir G, Cohen B, and Neeman M. Functional and molecular mapping of uncoupling between vascular permeability and loss of vascular maturation in ovarian carcinoma xenografts: the role of stroma cells in tumor angiogenesis. *Int J Cancer* 117: 202–211, 2005.
45. Gillies RJ, Bhujwalla ZM, Evelhoch J, Garwood M, Neeman M, Robinson SP, Sotak CH, and Van Der Sanden B. Applications of magnetic resonance in model systems: tumor biology and physiology. *Neoplas* 2: 139–151, 2000.
46. Golman K, Leunbach I, Ardenkjaer-Larsen JH, Ehnholm GJ, Wistrand LG, Petersson JS, Jarvi A, and Vahasalo S. Overhauser-enhanced MR imaging (OMRI). *Acta Radiolog* 39: 10–17, 1998.
47. Golman K, Petersson JS, Ardenkjaer–Larsen JH, Leunbach I, Wistrand LG, Ehnholm G, and Liu K. Dynamic *in vivo* oxymetry using overhauser enhanced MR imaging. *J Magn Reson* 12: 929–38, 2000.
48. Griffiths JR, Taylor NJ, Howe FA, Saunders MI, Robinson SP, Hoskin PJ, Powell ME, Thoumine M, Caine LA, and Baddeley H. The response of human tumors to carbogen breathing, monitored by Gradient-Recalled Echo Magnetic Resonance Imaging. *Int J Radiat Oncol Biol Phys* 39: 697–701, 1997.
49. Grubb RL, Jr., Raichle ME, Eichling JO, and Ter–Pogossian MM. The effects of changes in PaCO2 on cerebral blood volume, blood flow, and vascular mean transit time. *Stroke* 5: 630–639, 1974.
50. Hees PS and Sotak CH. Assessment of changes in murine tumor oxygenation in response to nicotinamide using 19F NMR relaxometry of a perfluorocarbon emulsion. *Magn Reson Med* 29: 303–310, 1993.
51. Heussel CP, Scholz A, Schmittner M, Laukemper–Ostendorf S, Schreiber WG, Ley S, Quintel M, Weiler N, Thelen M, and Kauczor HU. Measurements of alveolar pO_2 using ^{19}F-MRI in partial liquid ventilation. *Invest Radiol* 38: 635–641, 2003.
52. Hoge RD, Franceschini MA, Covolan RJ, Huppert T, Mandeville JB, and Boas DA. Simultaneous recording of task-induced changes in blood oxygenation, volume, and flow using diffuse optical imaging and arterial spin-labeling MRI. *Neuroimage* 25: 701–707, 2005.
53. Hou H, Khan N, O'Hara JA, Grinberg OY, Dunn JF, Abajian MA, Wilmot CM, Makki M, Demidenko E, Lu S, Steffen RP, and Swartz HM. Effect of RSR13, an allosteric hemoglobin modifier, on oxygenation in murine tumors: an *in vivo* electron paramagnetic resonance oximetry and bold MRI study. *Int J Radiat Oncol Biol Phys* 59: 834–843, 2004.
54. Howe FA, Robinson SP, and Griffiths JR. Modification of tumour perfusion and oxygenation monitored by gradient recalled echo MRI and 31P MRS. *NMR Biomed* 9: 208–216, 1996.
55. Hunjan S, Mason RP, Constantinescu A, Peschke P, Hahn EW, and Antich PP. Regional tumor oximetry: 19F NMR spectroscopy of hexafluorobenzene. *Int J Radiat Oncol Biol Phys* 41: 161–171, 1998.
56. Hyder F, Kida I, Behar KL, Kennan RP, Maciejewski PK, and Rothman DL. Quantitative functional imaging of the brain: towards mapping neuronal activity by BOLD fMRI. *NMR Biomed* 14: 413–431, 2001.
57. James PE, Bacic G, Grinberg OY, Goda F, Dunn JF, Jackson SK, and Swartz HM. Endotoxin induced changes in intrarenal pO_2 measured by *in vivo* electron paramagnetic resonance oximetry and magnetic resonance imaging. *Free Rad Biol Med* 21: 25–34, 1996.

58. Jelicks LA and Wittenberg BA. ^{1}H nuclear magnetic resonance studies of sarcoplasmic oxygenation in the red cell-perfused rat heart. *Biophys J* 68: 2129–2136, 1995.
59. Jezzard P, Heineman F, Taylor J, DesPres D, Wen H, Balaban RS, and Turner R. Comparison of EPI gradient-echo contrast changes in cat brain caused by respiratory challenges with direct simultaneous evaluation of cerebral oxygenation via a cranial window. *NMR Biomed* 7: 35–44, 1994.
60. Kida I and Hyder F. Physiology of functional magnetic resonance imaging: energetics and function. *Methods Mol Med* 124: 175–195, 2006.
61. Kleinschmidt A, Obrig H, Requardt M, Merboldt KD, Dirnagl U, Villringer A, and Frahm J. Simultaneous recording of cerebral blood oxygenation changes during brain activation by magnetic resonance imaging and near-infrared spectroscopy. *J Cereb Blood Flow Metab* 16: 817–826, 1996.
62. Koutcher JA, Alfieri AA, Devitt ML, Rhee JG, Kornblith AB, Mahmood U, Merchant TE, and Cowburn D. Quantitative changes in tumor metabolism, partial pressure of oxygen, and radiobiological oxygenation status postradiation. *Cancer Res* 52: 4620–4627, 1992.
63. Kreutzer U, Wang DS, and Jue T. Observing the ^{1}H NMR signal of the myoglobin Val-E11 in myocardium: an index of cellular oxygenation. *Proc Natl Acad Sci USA* 89: 4731–4733, 1992.
64. Krishna MC, Subramanian S, Kuppusamy P, and Mitchell JB. Magnetic resonance imaging for *in vivo* assessment of tissue oxygen concentration. *Sem Rad Oncol* 11: 58–69, 2001.
65. Kuethe DO, Caprihan A, Gach HM, Lowe IJ, and Fukushima E. Imaging obstructed ventilation with NMR using inert fluorinated gases. *J Appl Physiol* 88: 2279–2286, 2000.
66. Kupriyanov VV, Xiang B, Sun J, Dai G, Jilkina O, Dao V, and Deslauriers R. Three-dimensional (87)Rb NMR imaging and spectroscopy of K(+) fluxes in normal and postischemic pig hearts. *Magn Reson Med* 44: 83–91, 2000.
67. Kupriyanov VV, Xiang B, Yang L, and Deslauriers R. Lithium ion as a probe of Na+ channel activity in isolated rat hearts: a multinuclear NMR study. *NMR Biomed* 10: 271–276, 1997.
68. Kwong KK, Belliveau JW, Chesler DA, Goldberg IE, Weisskoff RM, Poncelet BP, Kennedy DN, Hoppel BE, Cohen MS, Turner R, and et al. Dynamic magnetic resonance imaging of human brain activity during primary sensory stimulation. *Proc Natl Acad Sci USA* 89: 5675–5679, 1992.
69. Lebon V, Brillault–Salvat C, Bloch G, Leroy–Willig A, and Carlier PG. Evidence of muscle BOLD effect revealed by simultaneous interleaved gradient-echo NMRI and myoglobin NMRS during leg ischemia. *Magn Reson Med* 40: 551–558, 1998.
70. Lebon V, Carlier PG, Brillault–Salvat C, and Leroy–Willig A. Simultaneous measurement of perfusion and oxygenation changes using a multiple gradient-echo sequence: application to human muscle study. *Magn Reson Imaging* 16: 721–729, 1998.
71. Ledermann HP, Schulte AC, Heidecker HG, Aschwanden M, Jager KA, Scheffler K, Steinbrich W, and Bilecen D. Blood oxygenation level-dependent magnetic resonance imaging of the skeletal muscle in patients with peripheral arterial occlusive disease. *Circul* 113: 2920–2935, 2006.
72. Lee SP, Duong TQ, Yang G, Iadecola C, and Kim SG. Relative changes of cerebral arterial and venous blood volumes during increased cerebral blood flow: implications for BOLD fMRI. *Magn Reson Med* 45: 791–800, 2001.
73. Lehmann F, Eberle B, Markstaller K, Gast KK, Schmiedeskamp J, Blumler P, Kauczor HU, and Schreiber WG. A software program for quantitative analysis of alveolar oxygen partial pressure paO_2 with oxygen-sensitive ^{3}He-MRI. *Rofo* 176: 1390–1398, 2004.
74. Lei H, Grinberg O, Nwaigwe CI, Hou HG, Williams H, Swartz HM, and Dunn JF. The effects of ketamine-xylazine anesthesia on cerebral blood flow and oxygenation observed using nuclear magnetic resonance perfusion imaging and electron paramagnetic resonance oximetry. *Brain Res* 913: 174–179, 2001.
75. Leniger–Follert E and Lubbers DW. Behavior of microflow and local PO2 of the brain cortex during and after direct electrical stimulation. A contribution to the problem of metabolic regulation of microcirculation in the brain. *Pflugers Arch* 366: 39–44, 1976.
76. Lindauer U, Gethmann J, Kuhl M, Kohl–Bareis M, and Dirnagl U. Neuronal activity-induced changes of local cerebral microvascular blood oxygenation in the rat: effect of systemic hyperoxia or hypoxia. *Brain Res* 975: 135–140, 2003.
77. Logothetis NK and Pfeuffer J. On the nature of the BOLD fMRI contrast mechanism. *Magn Reson Imaging* 22: 1517–1531, 2004.
78. Lurie DJ and Mader K. Monitoring drug delivery processes by EPR and related techniques—principles and applications. *Adv Drug Delivery Rev* 57: 1171–1190, 2005.
79. Ma J and Wehrli FW. Method for image-based measurement of the reversible and irreversible contribution to the transverse-relaxation rate. *J Magn Reson B* 111: 61–69, 1996.
80. Malisza KL, Kozlowski P, Ning G, Bascaramurty S, and Tuor UI. Metabolite changes in neonatal rat brain during and after cerebral hypoxia-ischemia: a magnetic resonance spectroscopic imaging study. *NMR Biomed* 12: 31–38, 1999.
81. Mason RP. Non-invasive assessment of kidney oxygenation: a role for BOLD MRI. *Kidney Int* 70: 10–11, 2006.
82. Mason RP, Rodbumrung W, and Antich PP. Hexafluorobenzene: a sensitive 19F NMR indicator of tumor oxygenation. *NMR Biomed* 9: 125–134, 1996.
83. Matcher SJ, Kirkpatrick P, Nahid K, Cope M, and Delpy DT. Absolute quantification methods in tissue near-infrared spectroscopy. *Proc SPIE* 2389: 486–495, 1995.
84. Matthews PM and Jezzard P. Functional magnetic resonance imaging. *J Neurol Neurosurg Psychiatry* 75: 6–12, 2004.
85. Mayevsky A, Nioka S, Subramanian VH, and Chance B. Brain oxidative metabolism of the newborn dog: correlation between 31P NMR spectroscopy and pyridine nucleotide redox state. *J Cereb Blood Flow Metab* 8: 201–207, 1988.
86. Menon RS, Ogawa S, Kim SG, Ellermann JM, Merkle H, Tank DW, and Ugurbil K. Functional brain mapping using magnetic resonance imaging. Signal changes accompanying visual stimulation. *Invest Radiol* 27 Suppl 2: S47–53, 1992.
87. Meyer RA, Towse TF, Reid RW, Jayaraman RC, Wiseman RW, and McCully KK. BOLD MRI mapping of transient hyperemia in skeletal muscle after single contractions. *NMR Biomed* 17: 392–398, 2004.
88. Muller TB, Sonnewald U, Westergaard N, Schousboe A, Petersen SB, and Unsgard G. 13C NMR spectroscopy study of cortical nerve cell cultures exposed to hypoxia. *J Neurosci Res* 38: 319–326, 1994.
89. Noseworthy MD, Bulte DP, and Alfonsi J. BOLD magnetic resonance imaging of skeletal muscle. *Sem Musculoskel Rad* 7: 307–315, 2003.
90. Noth U, Grohn P, Jork A, Zimmermann U, Haase A, and Lutz J. 19F-MRI *in vivo* determination of the partial oxygen pressure in perfluorocarbon-loaded alginate capsules implanted into the peritoneal cavity and different tissues. *Magn Reson Med* 42: 1039–1047, 1999.
91. Ogawa S, Lee T–M, Nayak AS, and Glynn P. Oxygenation-sensitive contrast in magnetic resonance image of rodent brain at high magnetic fields. *Magn Reson Med* 14: 68–78, 1990.
92. Ogawa S, Lee TM, Kay AR, and Tank DW. Brain magnetic resonance imaging with contrast dependent on blood oxygenation. *Proc Natl Acad Sci USA* 87: 9868–9872, 1990.
93. Ogawa S, Tank DW, Menon R, Ellermann JM, Kim SG, Merkle H, and Ugurbil K. Intrinsic signal changes accompanying sensory stimulation: functional brain mapping with magnetic resonance imaging. *Proc Natl Acad Sci USA* 89: 5951–5955, 1992.
94. Pauling L and Coryell CD. The magnetic properties and structure of hemoglobin, oxyhemoglobin and carbonmonoxyhemoglobin. *Proc Natl Acad Sci USA* 22: 210, 1936.
95. Payen JF, LeBars E, Wuyam B, Tropini B, Pepin JL, Levy P, and Decorps M. Lactate accumulation during moderate hypoxic hypoxia in neocortical rat brain. *J Cereb Blood Flow Metab* 16: 1345–1352, 1996.
96. Petersen ET, Zimine I, Ho YC, and Golay X. Non-invasive measurement of perfusion: a critical review of arterial spin labelling techniques. *Brit J Radiol* 79: 688–701, 2006.
97. Posse S, Kemna LJ, Elghahwagi B, Wiese S, and Kiselev VG. Effect of graded hypo- and hypercapnia on fMRI contrast in visual cortex: quantification of T(*)(2) changes by multiecho EPI. *Magn Reson Med* 46: 264–271, 2001.
98. Punwani S, Ordidge RJ, Cooper CE, Amess P, and Clemence M. MRI measurements of cerebral deoxyhaemoglobin concentration

[dHb]–correlation with near infrared spectroscopy (NIRS). *NMR Biomed* 11: 281–289, 1998.
99. Radda GK. Control of bioenergetics: from cells to man by phosphorus nuclear-magnetic-resonance spectroscopy. *Biochem Soc Trans* 14: 517–525, 1986.
100. Radford NB, Babcock EE, Richman A, Szczepaniak L, Malloy CR, and Sherry AD. 39K NMR measurement of intracellular potassium during ischemia in the perfused guinea pig heart. *Magn Reson Med* 40: 544–550, 1998.
101. Richardson RS, Duteil S, Wary C, Wray DW, Hoff J, and Carlier PG. Human skeletal muscle intracellular oxygenation: the impact of ambient oxygen availability. *J Physiol* 571: 415–424, 2006.
102. Robinson SP, Collingridge DR, Howe FA, Rodrigues LM, Chaplin DJ, and Griffiths JR. Tumour response to hypercapnia and hyperoxia monitored by FLOOD magnetic resonance imaging. *NMR Biomed* 12: 98–106, 1999.
103. Rolett EL, Azzawi A, Liu KJ, Yongbi MN, Swartz HM, and Dunn JF. Critical oxygen tension in rat brain: a combined 31P-NMR and EPR oximetry study. *Am J Physiol Cell Physiol* 279: R9–R16, 2000.
104. Schafer A, Jochimsen TH, and Moller HE. Functional magnetic resonance imaging with intermolecular double-quantum coherences at 3 T. *Magn Reson Med* 53: 1402–1408, 2005.
105. Schwarcz A, Natt O, Watanabe T, Boretius S, Frahm J, and Michaelis T. Localized proton MRS of cerebral metabolite profiles in different mouse strains. *Magn Reson Med* 49: 822–827, 2003.
106. Shu SK, Ashwal S, Holshouser BA, Nystrom G, and Hinshaw DB, Jr. Prognostic value of 1H-MRS in perinatal CNS insults. *Ped Neurol* 17: 309–318, 1997.
107. Silvennoinen MJ, Kettunen MI, and Kauppinen RA. Effects of hematocrit and oxygen saturation level on blood spin-lattice relaxation. *Magn Reson Med* 49: 568–571, 2003.
108. Sotak CH, Hees PS, Huang HN, Hung MH, Krespan CG, and Raynolds S. A new perfluorocarbon for use in fluorine-19 magnetic resonance imaging and spectroscopy. *Magn Reson Med* 29: 188–195, 1993.
109. Springett RJ, Wylezinska M, Cady EB, Hollis V, Cope M, and Delpy DT. The oxygen dependency of cerebral oxidative metabolism in the newborn piglet studied with ^{31}P NMRS and NIRS. *Adv Exp Med Biol* 530: 555–563, 2003.
110. Swartz HM, Bennett H, Brown III RD, Morse II PD, Pals M, and Koenig SH. Feasibility of measuring oxygen and redox metabolism *in vivo* by NMR: effect of paramagnetic materials and their cellular metabolism on relaxation times of protons of water and lipids. *Periodic Biologorum* 87: 175–183, 1985.
111. Swartz HM, Chen K, Pals M, Sentjurc M, and Morse PD. Hypoxia sensitive NMR contrast agents. *Magn Reson Med* 3: 169–174, 1986.
112. Tadamura E, Hatabu H, Li W, Prasad PV, and Edelman RR. Effect of oxygen inhalation on relaxation times in various tissues. *J Magn Reson Imaging* 7: 220–225, 1997.
113. Thomas SR, Pratt RG, Millard RW, Samaratunga RC, Shiferaw Y, McGoron AJ, and Tan KK. *In vivo* pO_2 imaging in the porcine model with perfluorocarbon F-19 NMR at low field. *Magn Reson Imaging* 14: 103–114, 1996.
114. Thulborn KR, Waterton JC, Mathews PM, and Radda GK. Oxygenation dependence of the transverse relaxation time of water protons in whole blood at high field. *Biochim Biophys Acta* 714: 265–270, 1982.
115. Thulborn KR, Watertown JC, and Radda GK. Proton imaging for *in vivo* blood flow and oxygen consumption measurements. *J Magn Reson* 45: 188–191, 1981.
116. Tran TK, Sailasuta N, Kreutzer U, Hurd R, Chung Y, Mole P, Kuno S, and Jue T. Comparative analysis of NMR and NIRS measurements of intracellular PO2 in human skeletal muscle. *Am J Physiol* 276: R1682–1690, 1999.
117. Tripathi A, Bydder GM, Hughes JM, Pennock JM, Goatcher A, Orr JS, Steiner RE, and Greenspan RH. Effect of oxygen tension on NMR spin-lattice relaxation rate of blood *in vivo*. *Invest Radiol* 19: 174–178, 1984.
118. Vaupel PW. Is there a critical tissue oxygen tension for bioenergetic status and cellular pH regulation in solid tumors? *Experientia* 52: 464-468, 1996.
119. Vink R. Nuclear magnetic resonance spectroscopy and the study of tissue oxygen metabolism: a review. *Adv Exp Med Biol* 316: 187–193, 1992.
120. Wang ZY, Noyszewski EA, and Leigh Jr. JS. *In vivo* MRS measurement of deoxymyoglobin in human forearms. *Magn Reson Med* 14: 562–567, 1990.
121. Warren WS, Ahn S, Mescher M, Garwood M, Ugurbil K, Richter W, Rizi RR, Hopkins J, and Leigh JS. MR imaging contrast enhancement based on intermolecular zero quantum coherences. *Science* 281: 247–251, 1998.
122. Wild JM, Fichele S, Woodhouse N, Paley MN, Kasuboski L, and van Beek EJ. 3D volume-localized pO_2 measurement in the human lung with ^{3}He MRI. *Magn Reson Med* 53: 1055–1064, 2005.
123. Wintermark M, Sesay M, Barbier E, Borbely K, Dillon WP, Eastwood JD, Glenn TC, Grandin CB, Pedraza S, Soustiel JF, Nariai T, Zaharchuk G, Caille JM, Dousset V, and Yonas H. Comparative overview of brain perfusion imaging techniques. *Stroke* 36: e83–99, 2005.
124. Wolber J, Cherubini A, Leach MO, and Bifone A. On the oxygenation-dependent (129)Xe T (1) in blood. *NMR Biomed* 13: 234–237, 2000.
125. Yablonskiy DA and Haacke EM. Theory of NMR signal behavior in magnetically inhomogeneous tissues: the static dephasing regime. *Magn Reson Med* 32: 749–763, 1994.
126. Yetkin FZ and Mendelsohn D. Hypoxia imaging in brain tumors. *Neuroimaging Clin N Am* 12: 537–552, 2002.
127. Zaharchuk G, Martin AJ, Rosenthal G, Manley GT, and Dillon WP. Measurement of cerebrospinal fluid oxygen partial pressure in humans using MRI. *Magn Reson Med* 54: 113–121, 2005.
128. Zhong J, Chen Z, Kwok WE, Kennedy S, and You Z. Optimization of blood oxygenation level-dependent sensitivity in magnetic resonance imaging using intermolecular double-quantum coherence. *J Magn Reson Imaging* 16: 733–740, 2002.
129. Zhong J, Kwok E, and Chen Z. fMRI of auditory stimulation with intermolecular double-quantum coherences (iDQCs) at 1.5T. *Magn Reson Med* 45: 356–364, 2001.

Address reprint requests to:
J.F. Dunn
Department of Radiology, Physiology and Biophysics
University of Calgary, Faculty of Medicine
3330 Hospital Drive NW
Calgary, Alberta
Canada, T2N 4N1

E-mail: dunnj@ucalgary.ca

Date of first submission to ARS Central, February 22, 2007; date of final revised submission, February 22, 2007; date of acceptance, March 8, 2007.

This article has been cited by:

1. Harold M. Swartz . 2007. On Tissue Oxygen and HypoxiaOn Tissue Oxygen and Hypoxia. *Antioxidants & Redox Signaling* **9**:8, 1111-1114. [Citation] [PDF] [PDF Plus]